ELSEVIER

Journal of Alloys and Compounds 316 (2001) 46–50

Journal of ALLOYS AND COMPOUNDS

www.elsevier.com/locate/jallcom

Transformations of magnetic phase diagram as a result of insertion of hydrogen and nitrogen atoms in crystalline lattice of $RFe_{11}Ti$ compounds

S.A. Nikitin[a,c,*], I.S. Tereshina[a,c], V.N. Verbetsky[b], A.A. Salamova[b]

[a]*Faculty of Physics, Moscow State University, Vorobyevy Gory, 119899 Moscow, Russia*
[b]*Faculty of Chemistry, Moscow State University, Vorobyevy Gory, 119899 Moscow, Russia*
[c]*International Laboratory of High Magnetic Fields and Low Temperatures, Gajowicka 95, 53-421, Wroclaw, Poland*

Received 26 September 2000; accepted 6 November 2000

Abstract

The effect of hydrogen and nitrogen insertions on the magnetic anisotropy and spin-reorientation transitions of $RFe_{11}Ti$ compounds have been studied. The obtained results are discussed on the basis of a model taking into account the interaction of the quadrupolar moment of the 4*f* rare earth ion shell with the electric field gradient produced not only by the charges of the ambient atom, but probably by the redistribution of states in the valence shells of the rare-earth ions and the conduction electron density. It is shown that the insertion of hydrogen and nitrogen atoms into the crystalline lattice of rare earth compounds provides control of both magnitude and sign of the magnetic anisotropy constants.

Keywords: Transition metal compounds; Rare earth compounds; Hydrogen absorbing materials; Magnetically ordered materials; Magnetic measurements

1. Introduction

The insertion of light interstitial elements (hydrogen, nitrogen, carbon) into the $RFe_{11}Ti$ (R=rare-earth metal) crystalline lattice results in an apparent change of their magnetic properties. Earlier [1,2] it was established that hydrides and nitrides retain the crystal structure ($ThMn_{12}$ type) of the parent alloys, though the atomic volume increases considerably resulting in a rise of Curie temperatures (T_C) and magnetisation. In the case of hydrides, T_C increases on average by 40–60 K. For nitrides T_C increases by 200–250 K. The change of the intra- and intersublattice exchange constants due to hydrogen insertion were estimated on the basis of the molecular field theory [3]. The saturation magnetisation of $RFe_{11}Ti$ increases on average by 5 and 14% for hydrides and nitrides, respectively.

Magnetic anisotropy phase diagrams have been obtained for $RFe_{11}Ti$ compounds generally from magnetically oriented powder samples [4]. It is well known that the most reliable data for the magnetic anisotropy can be obtained from measurements on single-crystal samples. Hitherto, no single crystals of the hydrogen containing compounds were available and so the researches of the effect of the insertion of elements on the magnetic anisotropy of $RFe_{11}Ti$ compounds containing various R-ions were insufficient.

The aim of the present paper was to study the influence of interstitial atoms on the magnetic anisotropy of $RFe_{11}TiH_x$ ($x=0$, 1) single crystals and aligned powder samples of $RFe_{11}TiN_x$ and to elucidate physical mechanisms responsible for the change of spin-reorientation transitions due to interstitial elements.

2. Experimental methods

The $RFe_{11}Ti$ polycrystalline samples (R=Y, Nd, Sm, Gd, Tb, Dy, Ho, Er, Yb, Lu) were prepared by induction melting under argon atmosphere of the constituent elements having a purity of at least 99.95 wt%. The ingots were crushed and remelted several times to ensure homogeneity. X-ray diffraction was used to control the single phase condition of the samples. Then the ingots were melted in an electric resistance furnace with a high temperature gradient and cooled slowly through the melting point in order to increase the grain size. Single crystals of $RFe_{11}Ti$ (except $NdFe_{11}Ti$) were extracted from the solidified ingots, weighing 2–20 mg, and were oriented by the conventional back Laue reflection method. Only the

*Corresponding author.
E-mail address: nikitin@rem.phys.msu.su (S.A. Nikitin).

0925-8388/01/$ – see front matter
PII: S0925-8388(00)01434-1

samples with subgrain disorientation less than 2–3° were used for the study.

Purified hydrogen obtained by decomposition of $LaNi_5H_x$ was used for hydrogenation. The single crystals were activated at $T=200$°C in a vacuum and then hydrogenated at the same temperature under a hydrogen pressure of 3×10^5 Pa for 2 h. Single crystals of the hydrogen containing compound $RFe_{11}TiH_{x-\delta}$ (except $NdFe_{11}Ti$ and $YbFe_{11}Ti$) were obtained without destruction of samples. The nitrides were formed by passing high-purity nitrogen gas at atmospheric pressure over fine powder samples (less than 10 μm) at 500°C for 4 h. The nitrogen and hydrogen content was estimated by determining the weight difference of the sample before and after nitrogenation and hydrogenation and by the volumetric method. The amount of absorbed H and N was 1 atom per $RFe_{11}Ti$ formula unit ($x\approx1$, δ about 0.05 or less). The nitrided powder were fixed in epoxy resin to form aligned samples of cylindrical shape in a magnetic field of 10 kOe. X-ray diffraction analysis was used to determine the structure both of the parent compounds and their hydrides and nitrides.

Magnetic measurements were performed on the single crystal hydrides $RFe_{11}TiH$ for R=Y, Sm, Gd, Tb, Dy, Ho, Er and Lu, and on magnetically oriented powder samples of $RFe_{11}TiN$ for R=Y, Sm, Tb, Dy with the aid of a pendulum and torque magnetometer in the temperature range 77–1000 K in magnetic fields up to 16 kOe. The standard equipment has been used at low temperature (4.2–100 K) in magnetic fields up to 150 kOe, produced with a superconducting coil (International Laboratory of High Magnetic Fields and Low Temperatures, Wroclaw, Poland). Magnetic anisotropy constants were determined from the fitting of magnetisation curves and from the torque angular dependence $L(\varphi)$ [5].

3. Results and discussion

Upon hydrogenation and nitrogenation the tetragonal symmetry of the parent compound is retained, but the lattice is expanded by more than ~1 and 3%, respectively. Crystallographic parameters (lattice constants *a* and *c*, unit cell volume *V*) are listed in Table 1. The hydrogen and nitrogen concentration: 1 atom per $RFe_{11}Ti$ formula unit, corresponds to full occupancy of the interstitial 2*b* site according to the neutron diffraction experiment [6,7] (see Fig. 1). This interstitial site can be seen as a pseudo-octahedron with two rare-earth ions and four iron atoms 8*j* at the corners. Interstitial atoms (hydrogen and nitrogen) occupy 2*b* sites adjacent to the rare earth, creating a change of crystal field that reflects the local symmetry and inducing significant changes of magnetic properties, especially of the magnetocrystalline anisotropy. Magnetic properties (saturation magnetization σ_S and anisotropy field H_A) are included in Table 1.

Fig. 2 indicates the magnetic structures found for $RFe_{11}Ti(H,N)_x$ compounds as a function of temperature. Magnetic phase diagrams constructed from the measurements of magnetic anisotropy constants show that both hydrogenation and nitrogenation have a considerable effect on the temperature intervals for the existence of either uniaxial magnetic states with an easy magnetisation direc-

Table 1
Crystallographic parameters and magnetic properties of $RFe_{11}Ti$ interstitial compounds

Compound	*a* (Å)	*c* (Å)	*V* (Å^3)	$\Delta V/V$ (%)	T_C (K)	σ_S (μ_B/f.u.)		H_a (kOe)	
						4.2 K	RT	4.2 K	RT
$YFe_{11}Ti$	8.509	4.783	346.6	–	538	18.8	16.1	40	20
$YFe_{11}TiH$	8.547	4.786	349.6	0.9	596	19.5	16.9	43	25
$YFe_{11}TiN$	8.610	4.801	355.9	2.7	742	21.2*	18.2	30	17
$NdFe_{11}Ti$	8.577	4.905	360.8	–	572	22.1	18.0	Cone	70
$SmFe_{11}Ti$	8.560	4.792	351.1	–	600	19.5	18.5	212	102
$SmFe_{11}TiH$	8.578	4.811	354.0	0.8	642	19.7	18.8	>250	150
$SmFe_{11}TiN$	8.646	4.816	360.1	2.6	746	21.3*	20	Plane	Plane
$GdFe_{11}Ti$	8.539	4.800	349.9	–	608	12.5	11.7	60	42
$GdFe_{11}TiH$	8.569	4.805	352.8	0.8	661	13.1	12.3	74	55
$TbFe_{11}Ti$	8.514	4.788	347.1	–	560	11.1	12.3	Plane	Plane
$TbFe_{11}TiH$	8.564	4.791	351.4	1.2	595	11.6	12.9	Plane	Plane
$TbFe_{11}TiN$	8.602	4.815	356.3	2.65	740	14.2*	14.1	120*	110
$DyFe_{11}Ti$	8.521	4.786	347.5	–	546	10	12	Plane	23
$DyFe_{11}TiH$	8.552	4.790	350.3	0.8	573	10.9	12.9	Plane	Cone
$DyFe_{11}TiN$	8.631	4.801	357.6	2.9	735	13.5*	13.4	130*	120
$HoFe_{11}Ti$	8.461	4.780	342.2	–	546	10.1	14.0	>70	30
$HoFe_{11}TiH$	8.502	4.781	345.6	1.0	561	10.6	14.7	Cone	35
$ErFe_{11}Ti$	8.480	4.775	343.4	–	507	11.3	14.4	Cone	28
$ErFe_{11}TiH$	8.507	4.781	346.0	0.8	563	11.8	15.1	Cone	31
$LuFe_{11}Ti$	8.448	4.768	340.3	–	490	19.5	17.2	42	40
$LuFe_{11}TiH$	8.479	4.791	344.4	1.2	545	21.2	18	54	46

*Values obtained at $T=77$ K.

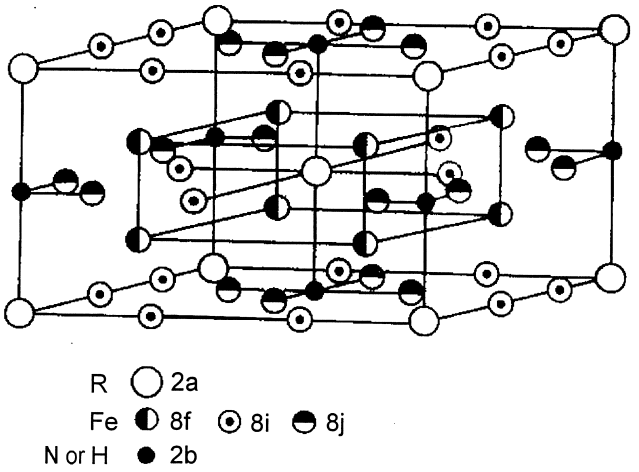

Fig. 1. Crystal structure of $RFe_{11}Ti(H, N)_x$ compounds according to neutron diffraction experiments [6,7].

tion (EMD) along the tetragonal *c*-axis or easy-plane states with EMD perpendicular to it.

It is seen from Fig. 2 that the introduction of hydrogen into the crystalline lattice of $TbFe_{11}Ti$ and $DyFe_{11}Ti$ induces easy plane states with magnetic moments $\mu \perp c$. Conversely, the introduction of hydrogen into the $SmFe_{11}Ti$ crystal lattice enhances its uniaxial anisotropy (according to our data $K_1 = 4.5 \times 10^7$ erg/cm^3 for $SmFe_{11}Ti$ and $K_1 = 4.8 \times 10^7$ erg/cm^3 for $SmFe_{11}TiH$ at $T = 300$ K).

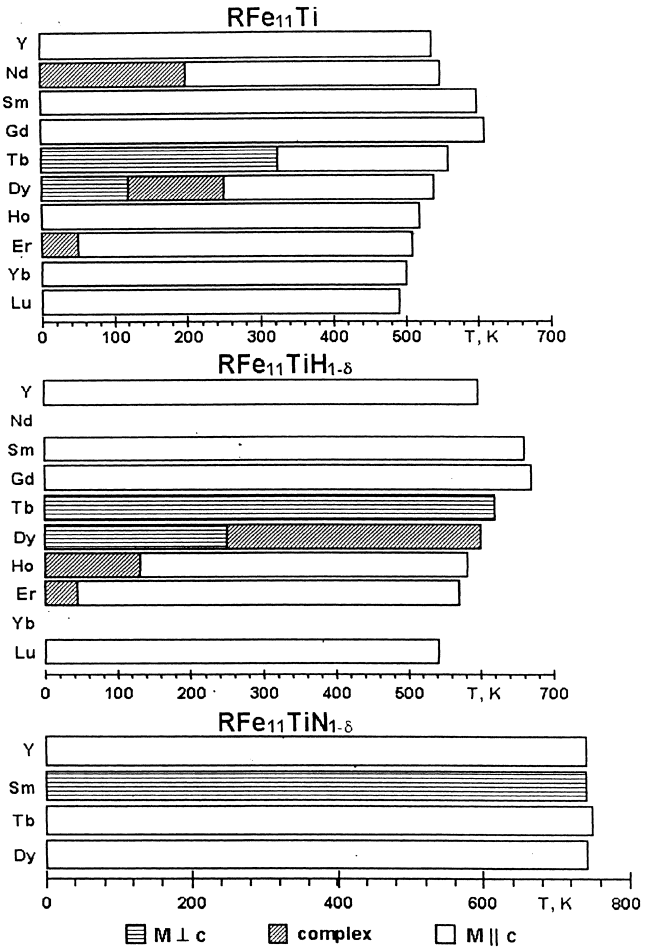

Fig. 2. Magnetic anisotropy phase diagrams of $RFe_{11}Ti(H, N)_x$ compounds.

The effects of hydrogen and nitrogen have an opposite effect on the magnetic anisotropy constants of the rare earth sublattice [8,9]. For example, the introduction of nitrogen atoms into the crystal lattice of $SmFe_{11}Ti$ results in an easy-plane compound $SmFe_{11}TiN$. In this connection one should mention the positive sign of the so-called second-order Stevens factor (α_J) for the Sm ion. It is well known, that at the rare-earth ions with $\alpha_J > 0$ (Sm, Er, Yb) the magnetic moment μ_R is parallel, while at the rare-earth ions with $\alpha_J < 0$ (Nd, Tb, Dy, Ho) it is perpendicular to the large axis of the 4*f*-electron charge cloud. In $TbFe_{11}Ti$ the anisotropy is of an easy-plane type for $T < 325$ K and uniaxial at $T > 325$ K. After hydrogenation the compound acquires an easy-plane anisotropy in the entire temperature range from 4.2 K to T_C, while after nitrogenation it becomes uniaxial and $K_1 = 4.0 \times 10^7$ erg/cm^3 at $T = 300$ K.

An explanation of the observed findings may be given on the basis of a model accounting for the electrostatic interaction of the quadrupolar moment of the 4*f* electronic shell with the electric field gradient. According to electrodynamics the interaction of a quadrupolar moment **q** with an electric field gradient $\nabla\mathbf{E}$ results in an energy [10]:

$$H = q\nabla E \tag{1}$$

In order to evaluate the energy of interaction of the quadrupolar moment **q** of the electronic 4*f* shell with an electric field gradient created by a neighboring ions and electrons, it is necessary to account for the interaction of the electric charge space distribution of the 4*f* electrons with a non-uniform electric field in a region, where the gradient $\nabla\mathbf{E}$ varies over the 4*f* electronic layer ($r_{4f} \sim 0.04$ nm, interatomic distances ~0.3 nm).

The electric field gradient at the position of the R ions occurs through the electrostatic interaction with the surrounding ions. Therefore it is necessary to take into account the hybridization of the 5*d* electrons of R ions with *s*- and *p*-electrons of the surrounding ions and the non-uniform electronic density distribution of the valence and conduction electrons [11–13]. It is very important that the interstitial atoms modify all the contributions to the electric field gradient.

The orientation of the aspherical change distribution of the 4*f* electrons with quadrupolar moment **q** is determined by the major axis of the 4*f* electron cloud. The latter is oriented with respect to the *c*-axis where the H and N ions are arranged in accordance with the sign of the electric field gradient $\nabla\mathbf{E}$ at the position of the R ion. Fig. 3 shows a schematic representation of the effect hydrogen and nitrogen on the quadrupolar moment **q** of the 4*f* shell and

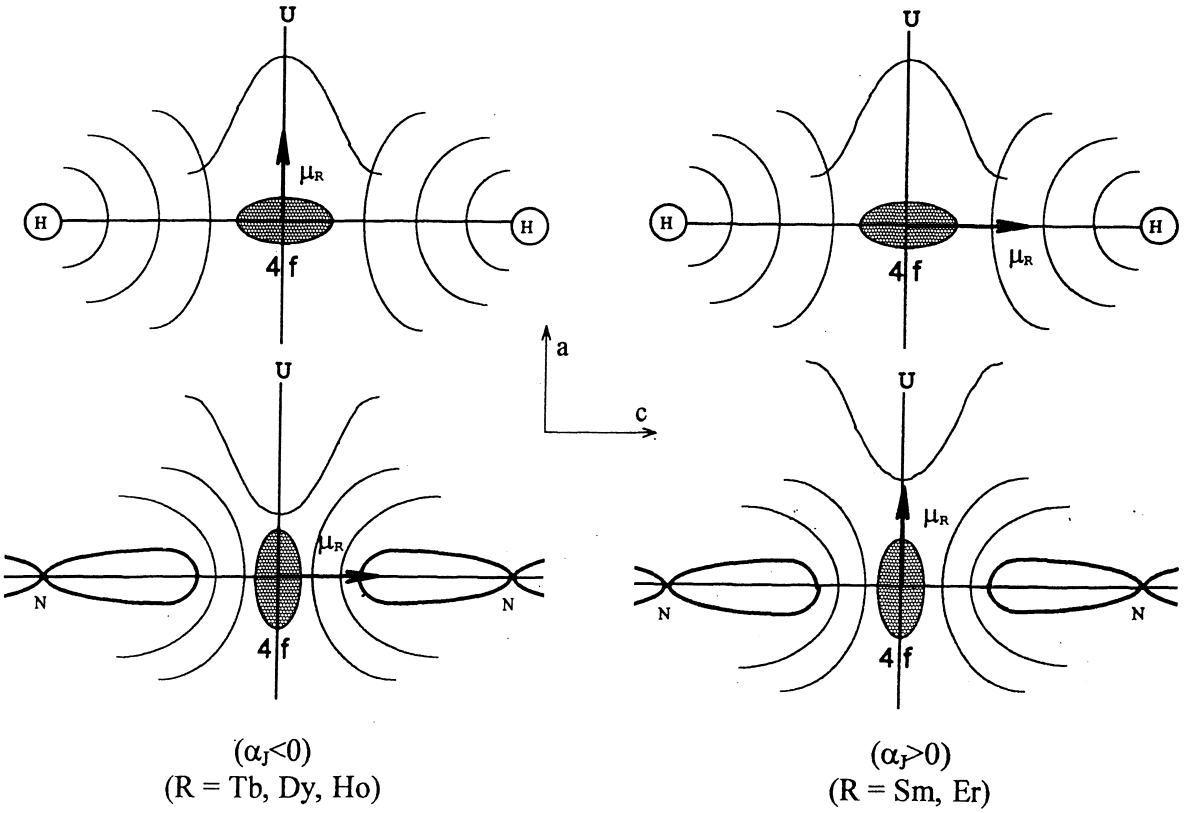

Fig. 3. Scheme of the interaction of quadrupolar and magnetic moments of 4*f* electron layer of rare earth ion with interstitial hydrogen and nitrogen atoms.

the magnetic moment μ_R of the R-ions in a non-uniform electric field. To simplify the discussion of the model shown in Fig. 3, let us introduce a local energy density $U = -\rho\varphi$, where ρ is the density of the negative 4*f* electron electric charge. Then making the assumption that in the first approximation the density within the 4*f* electron cloud of the rare earth ion is constant one obtains

$$\partial^2 U/\partial z^2 = +\rho\,\partial^2\varphi/\partial z^2 = \rho\nabla\mathbf{E} \quad (2)$$

where the coordinate z is measured along the tetragonal *c*-axis on which the interstitial H and N atoms are located.

The orientation of **q** will be corresponding to the energy minimum of the 4*f* quadrupole moment in the resultant electric field with a spatially non-uniform gradient $\nabla\mathbf{E}$.

For positive $\partial^2 U/\partial z^2$ (Fig. 3) **q** orients itself perpendicular to the *c*-axis. This implies $\mu_R \| \mathbf{c}$ for rare earths with negative Stevens coefficient ($\alpha_J < 0$) and $\mu_R \perp \mathbf{c}$ for $\alpha_J > 0$. For $\partial^2 U/\partial z^2 < 0$ **q** is parallel to the *c*-axis, while $\mu_R \perp \mathbf{c}$ for R ions with $\alpha_J < 0$ and $\mu_R \| \mathbf{c}$ for $\alpha_J > 0$.

The experimental spin-reorientation phase diagrams will be consistent with the proposed model if one assumes that the interstitial H and N atoms induce electric fields with opposite contributions to the $\nabla\mathbf{E}$. It is known [14] that nitrogen atoms conserve rigid 2*p* orbitals in metals, and are but weakly deformed by the crystal lattice, because the *p* electron is strongly coupled with the nitrogen anion. On the other hand, the electrons introduced by H atoms undergo hybridization without difficulty and move to the conduction band, which results in a non-uniform charge distribution of the conduction electrons [13]. Therefore the change of the electric field gradient at the position of R ions will be different for such dissimilar interstitial atoms as hydrogen and nitrogen when they are occupying the octahedral interstices.

Earlier [11] it was established that a renormalization of the asphericity of the valence electron charge cloud of the R atoms occurring as a consequence of hybridization with electron states of neighbouring atoms plays an important role in the theory of magnetic anisotropy. As a result the effective magnetic anisotropy constants are changed.

So the sign of the effect of interstitials on the magnetic anisotropy constants and SR transitions is determined by the following three factors: (i) the type of the interstitial atoms (it is an established fact that the interstitial effects are of different signs for nitrogen and hydrogen); (ii) the local surrounding of the R ions in $RFe_{11}Ti(H,N)_x$ crystals the positions of interstitial atoms are octahedral (2*b*) for $x \leq 1$, and tetrahedral for $x > 1$ (16*l* and 32*o*); (iii) the orientation of the quadrupole moment **q** of the asymmetric 4*f* shell with respect to the direction of the resulting magnetic moment of 4*f* electrons μ_R (for $\alpha_J > 0$ μ_R is oriented along the elongation direction of the space charge distribution of 4*f* electrons, and is perpendicular to it when

$\alpha_J < 0$). The change of the sign of first anisotropy constants with the introduction of interstitial atoms into the crystal lattice of $RFe_{11}Ti$ correlates with the sign of the Stevens factors. This illustrates the very important role of the orientation of the quadrupolar moment of rare earth 4*f* subshell relative to the crystal field.

Concluding, interstitial elements in the $RFe_{11}Ti$ crystal lattice provide effective means for controlling of both magnitude value and sign of the magnetic anisotropy constants.

Acknowledgements

The work has been supported by Federal Program on Support of Leading Scientific School Grant 00-15-96695 and RFBR Grant 99-02-17821.

References

[1] K.H.J. Buschow, in: Handbook of Magnetic Materials, Vol. 10, Elsevier, Amsterdam, 1997, p. 463.
[2] J.M.D. Coey, Rare-Earth Iron Permanent Magnets, Clarendon Press, Oxford, 1996.
[3] S.A. Nikitin, I.S. Tereshina, E.A. Ovtchenkov, V.N. Verbetsky, A.A. Salamova, Int. J. Hydrogen Energy (to be published).
[4] B.-P. Hu, H.-S. Li, J.P. Gavigan, J.M.D. Coey, J. Phys. Condens Matter. 1 (1989) 755–770.
[5] I.S. Tereshina, S.A. Nikitin, I.V. Telegina, V.V. Zubenko, Yu.G. Pastushenkov, K.P. Skokov, J. Alloys Comp. 283 (1999) 45–48.
[6] O. Isnard, S. Miraglia, M. Guillot, D. Fruchart, J. Alloys Comp. 275–277 (1998) 637–641.
[7] Y.C. Yang, L.S. Zhang, L.S. Kong, Q. Pan, S.L. Ge, J.L. Yang, Y.F. Ding, B.S. Zhang, C.T. Ye, Solid State Commun. 70 (10) (1991) 313–316.
[8] Y. Otani, D.P.F. Hurley, S. Hong, J.M.D. Coey, J. Appl. Phys. 69 (8) (1991) 5584–5589.
[9] S.A. Nikitin, E.A. Ovtchenkov, I.S. Tereshina, V.N. Verbetsky, A.A. Salamova, J. Magn. Magn. Mater. 195 (1999) 464–469.
[10] M.M. Bredov, V.V. Rumyantsev, I.N. Toptygin, in: Classical Electrodynamics, Nauka, Moscow, 1985, p. 102.
[11] R. Coehoorn, K.H.J. Buschow, M.W. Dirken, R.C. Thiel, Phys. Rev. B 42 (7) (1990) 4645–4652.
[12] P. Uebele, K. Hummler, M. Fähnle, Phys. Rev. B 53 (1996) 3296.
[13] V.Yu. Irkhin, Yu.P. Irkhin, Phys. Rev. B 57 (1998) 2697.
[14] V.K. Grigorovich, in: Metallic Bonding and Metal Structure, Nauka, Moscow, 1988, p. 296.